

Intrasubband magnetoplasmon LO-phonon coupling in an InAs antidot array

K. Bittkau,* C. Zehnder, Ch. Heyn, D. Heitmann, and C.-M. Hu

Institut für Angewandte Physik und Zentrum für Mikrostrukturforschung, Universität Hamburg, Jungiusstraße 11, 20355 Hamburg, Germany

(Received 14 May 2004; published 21 September 2004)

We present far-infrared photoconductivity measurements for InAs antidot arrays grown on a GaAs substrate. By applying a magnetic field, we have tuned the intraband-magnetoplasmon mode across the reststrahlen band of InAs. We have observed an anticrossing in the vicinity of the LO phonon of InAs arising from the intraband-magnetoplasmon-LO-phonon coupling. This coupling was so far only theoretically predicted. The experimentally observed splitting can be directly reproduced by the theory without any fitting parameters.

DOI: 10.1103/PhysRevB.70.125314

PACS number(s): 73.43.Lp, 73.50.Pz, 78.67.Hc

I. INTRODUCTION

There are many theoretical and experimental studies of the interaction of optical phonons and electrons in low-dimensional electron gases.¹⁻¹¹ In those works the interaction of the longitudinal optical (LO) phonons, in particular the polaron coupling, on the cyclotron resonance of a two-dimensional electron gas (2DEG) and the intersubband transition in 2DEG and quantum dots are studied. The impact of the optical phonons on the intrasubband magnetoplasmon is, to the best of our knowledge, only studied theoretically by Tselis *et al.*,² and more deeply by Peeters *et al.*⁴ and Wu.⁵ The experimental study of the electron-phonon interaction by transmission experiments is complicated due to the reduced transmission inside the reststrahlen band arising from the influence of the phonons on the dielectric properties.

In this paper, we present experimental results of the magnetoplasmon-LO-phonon coupling in an antidot array, which exhibits an anticrossing behavior. We show that this anticrossing can be perfectly described by the model of Tselis *et al.* without any fitting parameter.

We have performed far-infrared (FIR) photoconductivity (PC) measurements where the electron gas of an antidot array serves directly as the detector. This technique allows us to perform very sensitive measurements directly in the reststrahlen regime which is not accessible to transmission experiments. Therefore, the PC is an extremely sensitive technique to investigate the electron-phonon interaction.

We find that the bolometric effect is the origin of the PC in our samples.¹²⁻¹⁵ This effect arises from the heating of the electron gas due to the absorption of the FIR radiation and the temperature dependence of the longitudinal resistance of the sample.

II. THEORETICAL OVERVIEW

In the following, we would like to give a brief overview of the model we have used to calculate the magnetoplasmon-LO-phonon coupling in an antidot array.

Our antidot arrays are prepared by etching geometrical holes into an area of an InAs 2DEG grown on a GaAs substrate. In such an array there exists a periodically modulated electron gas, which allows us to excite intraband-

magnetoplasma oscillations with FIR radiation. This collective excitation differs from the corresponding mode in an unpatterned 2DEG. In the antidot array the collective modes can be described by a model of Mikhailov *et al.*,¹⁶

$$1 - \frac{(1-f)\omega_0^2}{\omega(\omega + \omega_c)} - \frac{f\omega_0^2}{\omega(\omega - \omega_c)} = 0, \quad (1)$$

where ω_0 is the excitation frequency of the magnetoplasmon mode for $B=0$ T and f the geometrical filling factor which defines the portion of the 2DEG area that is depleted by the geometrical holes. $\omega_c = eB/m^*$ is the cyclotron resonance. The fundamental collective excitations of an antidot array¹³ can be observed in our samples. One of these modes, the magnetoplasmon or ω^+ mode, approaches the optical phonon regime by increasing the magnetic field.

There are several processes that affect the interaction of phonons with low-dimensional electron systems. The magnetoplasmon-LO-phonon coupling is one example. These modes can be described for example by the equation given by Tselis *et al.*,²

$$\omega_{\pm}^2 = \frac{1}{2}(\omega_{mp}^2 + \omega_{LO}^2) \pm \frac{1}{2}\sqrt{(\omega_{mp}^2 + \omega_{LO}^2)^2 - 4(\omega_{LO}^2\omega_c^2 + \omega_p^2\omega_{TO}^2)}. \quad (2)$$

Here, ω_p and $\omega_{mp} = \sqrt{\omega_p^2 + \omega_c^2}$ are the frequencies of the plasmon and magnetoplasmon, respectively. In this theory, a continuous 2DEG is assumed with a constant electron density. For our antidot arrays, we have adopted this theory by the following replacements:

$$\omega_{mp} \rightarrow \omega^+, \quad \omega_p \rightarrow \sqrt{(\omega^+)^2 - \omega_c^2}. \quad (3)$$

The frequencies ω^+ and ω_c can be directly extracted from the experimental data.

III. SAMPLE STRUCTURE AND MEASUREMENT TECHNIQUE

Our samples were fabricated by molecular beam epitaxy on a GaAs substrate. To accommodate the lattice mismatch between GaAs and InAs, a multilayered buffer of $\text{In}_x\text{Al}_{1-x}\text{As}$ was grown where the In fraction was increased for each

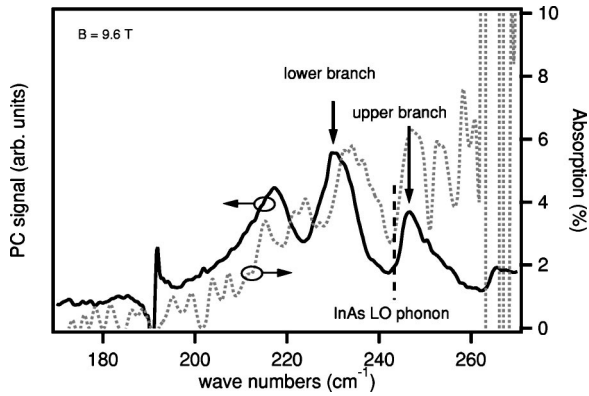


FIG. 1. Photoconductivity (solid curve) and absorption (dotted curve) spectrum of an antidot array at a magnetic field of 9.6 T. The PC spectrum was taken by applying a dc current of $9 \mu\text{A}$ at a sample temperature of 1.5 K. The arrows indicate the lower and upper branch of the magnetoplasmon-LO-phonon coupling at the InAs LO phonon (dashed line).

layer. A 7 nm thick Si-doped $\text{In}_{0.75}\text{Al}_{0.25}\text{As}$ layer was followed by a 5 nm spacer layer of $\text{In}_{0.75}\text{Al}_{0.25}\text{As}$. On the top of this structure, a step quantum well of a 2.5 nm $\text{In}_{0.75}\text{Ga}_{0.25}\text{As}$ layer, a 4 nm InAs layer and a 13.5 nm $\text{In}_{0.75}\text{Ga}_{0.25}\text{As}$ layer were grown. The samples were capped with a 40 nm thick layer of $\text{In}_{0.75}\text{Al}_{0.25}\text{As}$. A self-consistent Schrödinger-Poisson calculation shows that the 2DEG is about 55 nm below the surface, mainly confined in the narrow InAs channel.¹⁷

We prepared, by chemical wet etching, an extremely long Hall bar with a width of $W=50 \mu\text{m}$ and a length of about $L=10 \text{ cm}$. The 2DEG channel runs meandering in a square of $4 \times 4 \text{ mm}^2$. The large L/W ratio enhances the sensitivity of our measurement.

The antidot arrays had a period of 800 nm. The holes with a geometric diameter of about 200 nm were defined by holographical lithography and chemical wet etching. Ohmic contacts were prepared by depositing AuGe alloy followed by annealing. Further information about these samples can be found in Ref. 13.

Our experiment was performed by applying a dc current to the Hall bar and measuring the changes of the voltage drop caused by the FIR radiation. At fixed magnetic fields, the broadband FIR radiation was modulated by the Michelson interferometer of a Fourier transform spectrometer. Using the sample itself as the detector, the corresponding change in the voltage drop of the sample was ac coupled to a broadband preamplifier and recorded as an interferogram which was Fourier transformed to extract the photoconductivity spectrum. The sample was mounted in a He cryostat with a superconducting solenoid. All data reported here were obtained in Faraday geometry.

IV. EXPERIMENTAL RESULTS

Figure 1 shows the photoconductivity (PC) and absorption spectrum of an antidot array at a magnetic field of $B=9.6 \text{ T}$. The PC spectrum was taken by applying a dc current of $9 \mu\text{A}$ at a sample temperature of $T=1.5 \text{ K}$. The total in-

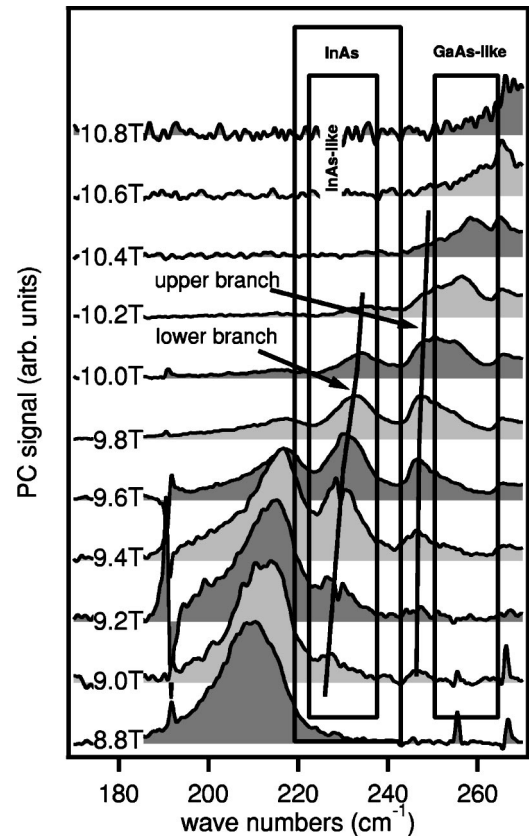


FIG. 2. Overview of photoconductivity spectra in the regime of the optical phonons. The reststrahlen bands of InAs and InGaAs are indicated by the rectangles. The lower and upper branch of the magnetoplasmon-LO-phonon coupling are shown by the black lines as guide to the eyes. The spectra are vertically offset for clarity.

tensity of the PC depends on the Landau filling factor. One can see several resonances in the spectrum arising from the influence of the optical phonon modes of the different materials. We observe two peaks in the vicinity of the LO phonon of InAs (dashed line). These two modes represent, as we justify later, the lower and upper branch of the magnetoplasmon-LO-phonon coupling, which exhibits an anticrossing behavior. By comparison with the absorption spectrum one can see the advantage of the photoconductivity technique. Because of the reduced transmission in the vicinity of the optical phonons, the signal to noise ratio of the absorption spectrum is very low and the identification of resonances difficult.

In Fig. 2 different photoconductivity spectra of the antidot array are shown. The spectra are taken in a magnetic field regime where the magnetoplasmon resonance lies inside the reststrahlen band of InAs. Because of the filling factor dependence of the PC intensity, each spectrum is divided by a factor to facilitate a comparison. One can clearly see the anticrossing in the vicinity of the InAs LO phonon arising from the magnetoplasmon-LO-phonon coupling. The lower and upper branches of this coupling are shown by the black lines. Here and in the following, the rectangles represent the reststrahlen bands of InAs and InGaAs. The energies of the TO (LO) phonon modes of InAs are 218.9 cm^{-1} (243.3 cm^{-1}).¹⁸ In the ternary mixed crystal of $\text{In}_{0.75}\text{Ga}_{0.25}\text{As}$

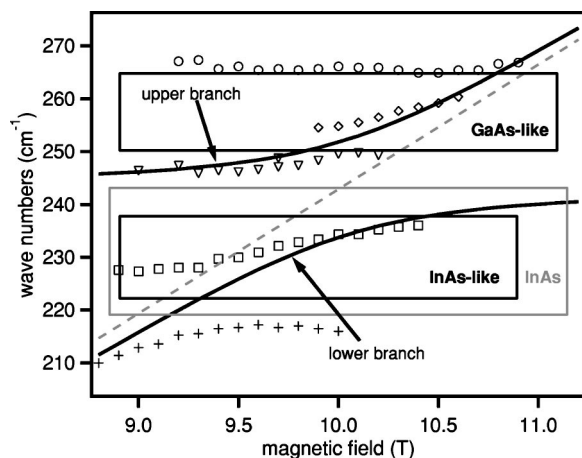


FIG. 3. Experimental magnetic field dispersion for the antidot array (symbols). The calculated magnetoplasmon-LO-phonon modes are shown as solid lines. The “bare” magnetoplasmon mode is shown as a dashed line in addition. The rectangles indicate the reststrahlen bands of InAs and InGaAs.

there exist two reststrahlen bands¹⁹ with InAs-like and GaAs-like phonon modes. The energies of the TO (LO) phonon are 222 cm^{-1} (238 cm^{-1}) for the InAs-like modes and 250 cm^{-1} (265 cm^{-1}) for the GaAs-like modes.

V. DISCUSSION

In Fig. 3 we have plotted the peak positions of the experimentally observed resonances for the different branches with different symbols and observe a clear anticrossing at the InAs LO-phonon frequency. To compare these experimental results with theory we have used the model described in Sec. II. The two branches of the calculated magnetoplasmon-LO-phonon coupling are shown in the magnetic field dispersion as solid lines. The “bare” magnetoplasmon mode ω^+ of the antidot array is depicted as a dashed line in addition. One finds an excellent agreement of the anticrossing around the LO phonon mode of InAs without any fitting parameter.

In principle, a polaron-like coupling with the LO phonon would also give rise to an anticrossing at the LO-phonon frequency. To check this we have performed PC measurements on an unpatterned sample from the same wafer. In-

stead of the magnetoplasma oscillation one observes the cyclotron resonance in this sample, which shows no anticrossing behavior around the LO-phonon frequency of InAs. This screening of the polaron effect is due to the large carrier density in our samples.^{6,7} Since the unpatterned and antidot samples have only slightly different densities, we would expect that the polaron coupling in the antidot sample is similarly weak. Therefore, we can rule out the polaron coupling to be the origin of the anticrossing around the InAs LO phonon in our antidot arrays. Because of this and the perfect parameter free fit with the theory we conclude that this anticrossing is the manifestation of the intraband-magnetoplasmon-LO-phonon coupling.

In the following, we would like to discuss briefly some further splittings that we observe in the experiments. In particular, one can see splittings around both the InAs-like and GaAs-like TO phonon frequencies. These splittings arise from macroscopic dielectric effects.²⁰ They reflect the strong variation of the dielectric function in the vicinity of the optical phonons. We have performed dielectric calculations using the transfer matrix method for a multilayered structure. In this model, the absorption of the cyclotron resonance of a 2DEG is taken into account. We find that the additional splittings at the TO phonon frequencies can be fully explained by the dielectric calculations, in particular the damping of the radiation in the vicinity of the TO phonons.

VI. SUMMARY

In summary, we have observed an anticrossing behavior of the intraband magnetoplasmon in the vicinity of the InAs LO phonon. We clearly observed a lower and upper branch, which can be excellently described by the magnetoplasmon-LO-phonon coupling with the model of, e.g., Tselis *et al.* This coupling was, to the best of our knowledge, never observed experimentally before. We can rule out the polaron coupling to be the origin of the anticrossing from corresponding measurements on an unpatterned 2DEG.

ACKNOWLEDGMENTS

We gratefully acknowledge the support of this work by the EU through project BMR, the BMBF through Project No. 01BM905 and the DFG through SFB 508 and the Graduiertenkolleg “Physik nanostrukturierter Festkörper.”

*Electronic address: kbittkau@physnet.uni-hamburg.de

¹M. Horst, U. Merkt, and J. P. Kotthaus, Phys. Rev. Lett. **50**, 754 (1983).

²A. C. Tselis and J. J. Quinn, Phys. Rev. B **29**, 3318 (1984); H. C. A. Oji and A. H. MacDonald, *ibid.* **34**, 1371 (1986).

³H. Sigg, P. Wyder, and J. A. A. J. Perenboom, Phys. Rev. B **31**, 5253 (1985).

⁴F. M. Peeters, X. Wu, and J. T. Devreese, Phys. Rev. B **36**, 7518 (1987).

⁵X. Wu, Phys. Rev. B **38**, 4212 (1988).

⁶C. J. G. M. Langerak, J. Singleton, P. J. van der Wel, J. A. A. J. Perenboom, D. J. Barnes, R. J. Nicholas, M. A. Hopkins, and C. T. B. Foxon, Phys. Rev. B **38**, 13133 (1988).

⁷F. M. Peeters, X.-G. Wu, J. T. Devreese, C. J. G. M. Langerak, J. Singleton, D. J. Barnes, and R. J. Nicholas, Phys. Rev. B **45**, 4296 (1992).

⁸C.-M. Hu, E. Batke, K. Köhler, and P. Ganser, Phys. Rev. Lett. **75**, 918 (1995); **76**, 1904 (1996).

⁹X. G. Wu, F. M. Peeters, Y. J. Wang, and B. D. McCombe, Phys. Rev. Lett. **84**, 4934 (2000).

- ¹⁰S. Hameau, J. N. Isaia, Y. Guldner, E. Deleporte, O. Verzellen, R. Ferreira, G. Bastard, J. Zeman, and J. M. Gérard, *Phys. Rev. B* **65**, 085316 (2002); S. Hameau, Y. Guldner, O. Verzellen, R. Ferreira, G. Bastard, J. Zeman, A. Lemaitre, and J. M. Gérard, *Phys. Rev. Lett.* **83**, 4152 (1999).
- ¹¹L. V. Kulik, I. V. Kukushkin, V. E. Kirpichev, S. V. Tovstonog, V. E. Bisti, K. von Klitzing, and K. Eberl, *J. Exp. Theor. Phys.* **95**, 927 (2002).
- ¹²C.-M. Hu, C. Zehnder, Ch. Heyn, and D. Heitmann, *Phys. Rev. B* **67**, 201302(R) (2003).
- ¹³K. Bittkau, Ch. Menk, Ch. Heyn, D. Heitmann, and C.-M. Hu, *Phys. Rev. B* **68**, 195303 (2003).
- ¹⁴C. Zehnder, A. Wirthmann, Ch. Heyn, D. Heitmann, and C.-M. Hu, *Europhys. Lett.* **63**, 576 (2003).
- ¹⁵F. Neppel, J. P. Kotthaus, and J. F. Koch, *Phys. Rev. B* **19**, 5240 (1979); K. Hirakawa, K. Yamanaka, Y. Kawaguchi, M. Endo, M. Saeki, and S. Komiyama, *ibid.* **63**, 085320 (2001).
- ¹⁶S. A. Mikhailov and V. A. Volkov, *Phys. Rev. B* **52**, 17260 (1995); S. A. Mikhailov, *ibid.* **54**, R14293 (1996).
- ¹⁷A. Richter, M. Koch, T. Matsuyama, Ch. Heyn, and U. Merkt, *Appl. Phys. Lett.* **77**, 3227 (2000).
- ¹⁸M. Hass and B. W. Hennis, *J. Phys. Chem. Solids* **23**, 1099 (1962).
- ¹⁹M. H. Brodsky and G. Lucovsky, *Phys. Rev. Lett.* **21**, 990 (1968).
- ²⁰M. Ziesmann, D. Heitmann, and L. L. Chang, *Phys. Rev. B* **35**, 4541 (1987).